Modelling Foil Winding Configurations with Low AC and DC Resistance

J. D. Pollock
C. R. Sullivan

Found in *IEEE Power Electronics Specialists Conference,* June 2005, pp. 1507–1512.

Modelling Foil Winding Configurations with Low AC and DC Resistance

Jennifer D. Pollock and Charles R. Sullivan
jennifer.pollock@dartmouth.edu charles.r.sullivan@dartmouth.edu http://power.thayer.dartmouth.edu
8000 Cummings Hall, Dartmouth College, Hanover, NH 03755, USA

Abstract— **Significant reductions in winding losses can be achieved by modifying the shape of the cross section of a foil winding. A new method provides improved accuracy for loss calculation in windings with semi-circular cut-outs on gapped cores, as verified by experimental measurements. Optimization using this loss calculation produces designs with up to a factor of two lower losses than either full-width foil windings or litz-wire windings. Foil winding shapes for distributed-gap cores are also introduced and shown to provide reduction in power loss.**

I. Introduction

BECAUSE of their low dc resistance, foil windings are commonly used in inductors that must handle a large dc current. However, the current is rarely just a dc current, but usually has some ac ripple riding on it, and thus the ac resistance of the winding becomes important. For example, the inductors in many dc-dc converter circuits handle a current waveform composed of a large dc component with some ac ripple at the switching frequency riding on it. In multilayer windings, ac loss can be proportional to the number of turns squared, so even if the ripple is small compared to the dc current, a large ac resistance can result in large ac losses. The ac resistance in foil windings can seriously degrade the overall performance and outweigh the benefits of the low dc resistance. This paper develops an optimization method to reduce the ac resistance of foil windings while maintaining a low dc resistance. This is accomplished by adjusting the size and shape of the winding cross section to optimize the tradeoff between ac and dc power loss.

Previous work done on reducing the ac resistance of inductor windings by optimizing the winding shape has addressed round-wire or litz-wire windings [1], [2], [3], but little work has addressed shape-optimized foil inductor windings. In [4], foil windings are shaped to match the flux lines created by a gapped high-permeability core. Although the method in [4] could be very effective in reducing losses, it is not practical to construct windings in the complex shapes that are proposed. In [5], [6], foil windings for gapped-inductors are notched by removing copper from the region near the air-gap in the core. The tradeoff between ac and dc loss was evaluated to find the optimum shape of the cross-section that gives the lowest total loss. The optimum notch shape was determined to be semi circular, based on finite element analysis (FEA). The current distribution around the surface of the notch is approximately uniform, which can be explained by the equal distance from the end of each layer to the gap. The power loss calculation used in [5] is not accurate because it is based on a simplified calculation that does not match the power loss determined by FEA. The power loss calculation was used in the size optimization method to determine the optimum size of the notch in the foil. Because the power loss calculation is only an estimate of actual power loss, the optimization method does not determine the true optimal notch size. However, the optimal designs predicted still had improved performance, i.e lower total loss, than the full-width foil windings.

This work was supported in part by the United States Department of Energy under grant DE-FC36-01GO1106

In this paper, an improved method for the power loss calculation used in the optimization of gapped-inductor foil windings is presented. The power loss predicted by the optimization method closely matches both the finite element analysis (FEA) and experimental results. In addition, we introduce a new foil winding shape that can provide similar ac-resistance improvements for a distributed-gap core.

Power loss calculations used by the optimization method for the gapped, high-permeability inductor are developed in Section II-A – II-C. The results of the optimization method are presented in Section II-D. The power loss calculations are verified in Section II-E. Section III contains a discussion of possible foil winding shapes for distributed-gap inductors. In Section III-A, the performance of the new distributed gap winding configurations are verified with numerical field simulations and the results are discussed.

II. Optimization

An optimization program to design shaped foil windings was developed in MATLAB [7]. The optimization determines the radius of a semi-circular cutout to minimize power losses for a winding on a gapped high-permeability core. In order to develop an optimization, a simple but accurate loss calculation method is needed.

A. Modelling Notched Foil Windings

The total power loss is calculated by summing the ac and dc loss components. The dc component of loss is calculated by $P_{dc} = I_{dc}^2 R_{dc}$, where the dc resistance, R_{dc}, is equal to $R_{dc} = \sum_{i=1}^{N} \frac{\rho l_i}{A_{dc,i}}$ where $A_{dc,i}$ is the cross-sectional area of the i^{th} layer, l_i is its length, and ρ is the resistivity of copper.

The ac power loss is computed for each harmonic of the ripple frequency and then summed to give the total ac power loss,

$$P_{ac,total} = \Sigma I_{rms,j}^2 R_{ac,j} \quad (1)$$

where $I_{rms,j}$ is the RMS amplitude of the current for the j^{th} harmonic and $R_{ac,j}$ is the resistance for the j^{th} harmonic. A method for estimating the ac resistance is outlined below.

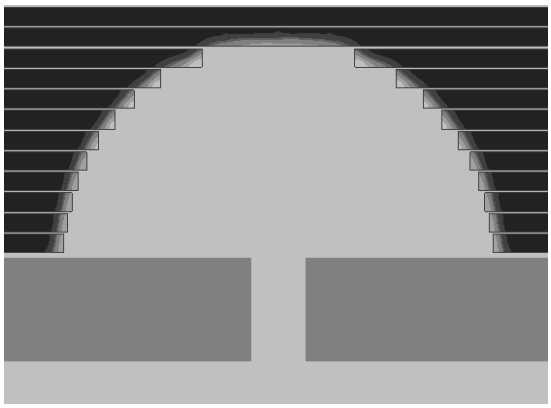

Fig. 1. This figure shows the current distribution in a circular-notched foil winding with a gapped, high-permeability core.

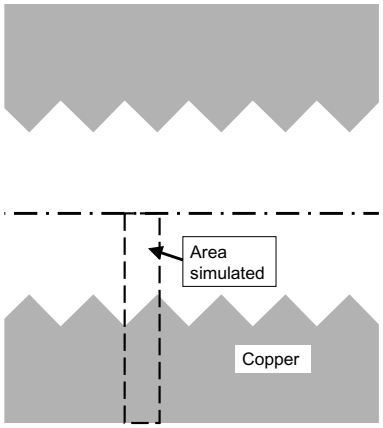

Fig. 2. The simple model simulated to better understand the current crowding in corners of foil layers. The area in the dash box was simulated.

The current distribution for a circular notch cutout, from a finite-element simulation, is shown in Fig. 1. Most of the current flows on the surface of the notch. Ideally, all the current would flow on the surface of the notch, but this not the case, especially when the notch does not expose an area of each layer to the air gap. Currents that flow along other surfaces of the foil tend to be uniformly distributed across the top and/or bottom surfaces of the foils. These internal currents induce eddy currents in the layers between where the current produces the MMF and the air-gap where the MMF is dropped. Thus, the calculation of internal currents and the corresponding losses is complicated by proximity effect, although it can also be simplified by using a one-dimensional model. The loss due to the currents on the surface of the notch, P_s, is calculated separately from the loss due to internal currents.

In order to determine the ac resistance, a unit current is applied to the winding as a thought experiment. The ac resistance determined from this unit-current excitation can then be used in (1) to calculate power loss with the actual current waveforms. The method presented here to determine the ac resistance of a notched foil winding is done for sinusoids at each frequency. The surface power loss (the loss due to the surface currents) and internal power loss (the loss due to internal currents) are calculated based on the unit current. The total current in the cross section of each layer must equal the terminal current:

$$I = I_s + I_{int} \tag{2}$$

where I_s is the surface current, I_{int} is the internal current and I is the terminal current, in this case a unit test current. The surface current for each layer is determined by the ratio of the arc length of the edge, $\ell_{e,i}$ of the i^{th} layer exposed the air gap to the total arc length of all layers exposed to the air gap.

$$I_{s,i} = \frac{\ell_{e,i}}{\sum_{i=1}^{N} \ell_{e,i}} NI \tag{3}$$

where N is the number of turns in the winding.

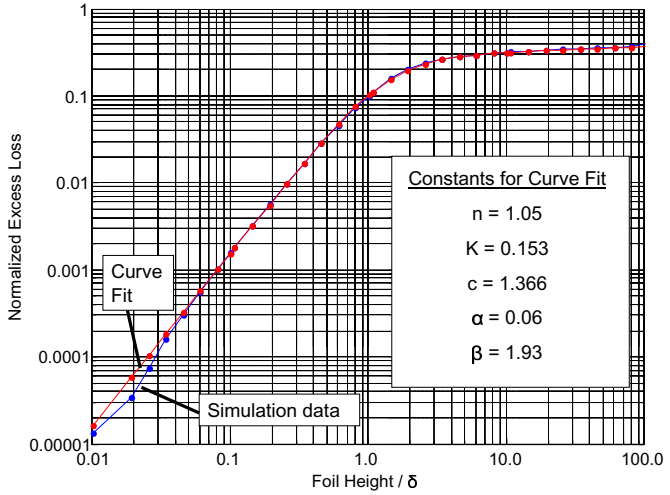

Fig. 3. The normalized excess loss versus the ratio of foil height to δ for the simulation data. The curve fit to the data by (3) is also shown with the constants used to fit the function to the data.

B. Surface Power Loss Estimation

The power loss due to the surface currents is determined by approximating the area where the surface current flows. The surface area, $A_{s,i}$ for the i^{th} layer is:

$$A_{s,i} = \ell_{e,i}\delta \tag{4}$$

where δ is the skin depth given by $\delta = \sqrt{2\rho/\omega\mu_0}$ and ρ is the resistivity of copper, ω is the radian frequency and μ_0 is the permeability of free space.

The approximate surface power loss, $\tilde{P}_s$, can be calculated from

$$\tilde{P}_s = I^2 N^2 \frac{\rho \ell_t}{A_s} \tag{5}$$

where ℓ_t is the mean length of a turn and $A_s = \sum_{i=1}^{N} A_{s,i}$.

$\tilde{P}_s$ underestimates the actual surface power loss. We believe this is due to the current crowding the corners of each foil layer. This effect can be seen in Fig. 1. So, we set out to determine a

surface loss factor that would adjust the surface loss calculated by (5) to match the surface loss predicted by FEA. Fig. 2 shows a simplified model of a conductor with steps in it, which are analogous to the steps created by the layers of foil in the actual winding that was used to model the current crowding effect. A wide range of ratios between foil height and skin depth, X, was examined. The power loss, P_s, for each was determined by FEA for the section outlined by the dashed rectangle in Fig. 2. Excess loss, P_{excess}, is defined as:

$$P_{excess} = P_s - \tilde{P}_s. \tag{6}$$

The excess loss, estimated by FEA, is normalized to the approximate surface loss calculated by (5), and plotted verses the ratio of foil height to skin depth in Fig. 3. A dual-slope function [8] was used to fit a curve to the data:

$$\hat{P}_{excess}(X) = \frac{KX^{\alpha}}{(X^{-\beta n} + c^{-\beta n})^{\frac{1}{n}}}. \tag{7}$$

The constant c controls the point at which the transition between slopes occurs. n determines whether the transition is abrupt (large values of n) or smooth (small values of n). The constants K, α and β were chosen to fit (7) to the simulation data. The value used for each constant is shown in Fig. 3.

The curve fit to normalized excess loss, $\hat{P}_{excess}(X)$, must be adjusted because it was developed for a uniform cutout where the foil height and step size are equal and we wish to apply it to a circular cutout. The step size for each layer varies for the circular cutout, so to account for this we use half of $\hat{P}_{excess}(X)$. This will overestimate the loss for the layers where the step size is less than the foil height and underestimate it for the layers where the step size larger than the foil height. The corrected estimate of surface loss, $\hat{P}_s$, is then:

$$\hat{P}_s = \tilde{P}_s \left(1 + \frac{\hat{P}_{excess}(X)}{2}\right). \tag{8}$$

C. Internal Power Loss Estimation

The internal power loss was calculated using the one-dimensional solutions to Maxwell's equations. The loss per unit length, P_l, resulting from the one-dimensional solution for a conductive layer with known fields on either side is conveniently expressed in [9].

$$P_l = \frac{1}{2}\frac{b\rho}{\delta}\left[(H_a - H_b)^2 F(h/\delta) + 2H_a H_b G(h/\delta)\right] \tag{9}$$

where b is the width of foil, h is the thickness of foil, ρ is the resistivity of conductor, H_a is the magnetic field on one side of conductor and H_b is the magnetic field on the other side of conductor. The functions $F(x)$ and $G(x)$ are $F(x) = \frac{\sinh(2x)+\sin(2x)}{\cosh(2x)-\cos(2x)}$ and $G(x) = \frac{\sin(x)-\sinh(x)}{\cosh(x)+\cos(x)}$. To calculate the magnetic fields on the surfaces of the foils, we start by considering the field on the surface of the first layer next to the core, $H_{a,1}$. Except in the notched region near the gap, the foil is close enough to the high-permeability core that we can consider the field at its surface to be approximately zero; $H_{a,1} = 0$. By Ampere's law, the field at the opposite side of the same foil is

$$H_{b,1} = \frac{I_{int,1}}{b_1} \tag{10}$$

where $I_{1,int}$ is the internal current in the first layer and b_1 is the width of the foil (not including the notched portion). To calculate the field at the surfaces of the following layers, we use $H_{a,i+1} = H_{b,i}$ and follow the same approach to find the field between subsequent layers

$$H_{a,k} = \frac{\sum_{i=1}^{k} I_{int,i}}{b_k}. \tag{11}$$

TABLE I
INDUCTOR SPECIFICATIONS

Specification	Value	Units
Inductance	70	uH
Number of Turns, N	15	NA
DC current, I_{dc}	40	A
Peak-to-Peak Ripple Amplitude	6	A
Ripple Frequency	50	kHz
Core	E71/33/32 in Thomson B2 material	NA

D. Optimization Results

Given the method for the calculation of power loss in Section II-A - Section II-C, standard numerical optimization algorithms can be used to find the optimum value of the radius used to describe the shape of the notch in the winding as shown in Fig. 1 to minimize total loss. We used the Nelder-Mead simplex algorithm as implemented in the MATLAB function fminsearch [10].

The optimization program was used to determine the winding design with the lowest total loss for the inductor detailed in Table I at several ripple ratios, where ripple ratio is defined as:

$$r_r = \frac{I_{ac_{pp}}}{I_{dc}}. \tag{12}$$

The results of the optimization program are shown in Fig. 4. Each point on the optimization curve represents a different size notch, optimized for that ripple ratio. The designs chosen by the optimization program were simulated using FEA to confirm the accuracy of the loss calculations in Section II-A – II-C; we can see that the loss calculation works very well.

It is clear from Fig. 4 that the notched foil can offer substantial improvements compared to a full-bobbin foil design. However, other techniques can be used to achieve decreased ac resistance, such as spacing a full-width foil winding away from the gap, or using litz wire. Thus, to determine whether the notched foil design is in fact better than any of these alternatives, and if so, for what situations, curves for optimized designs using litz wire or foil spaced away from the gap are also included in Fig. 4.

The program used to optimize the litz-wire windings [11] provides a range of different designs for each ripple ratio, each with a different cost/loss tradeoff. In Fig. 4, we include only the lowest loss design, despite its high cost. Another way to reduce ac loss in foil windings is to move the winding away from the

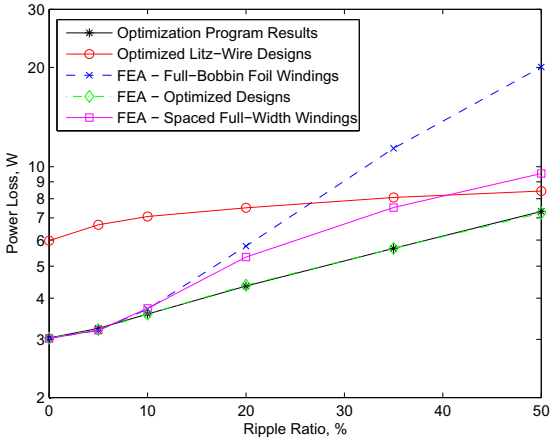

Fig. 4. Results of optimization. The full-width foil is compared to the optimized notched foil, optimized litz-wire winding and space full-width foil winding for a gapped, high-permeability core. At 20% ripple, the losses in the notched foil winding are 18% less than the space full-width foil winding design and 31% less than the full-width foil.

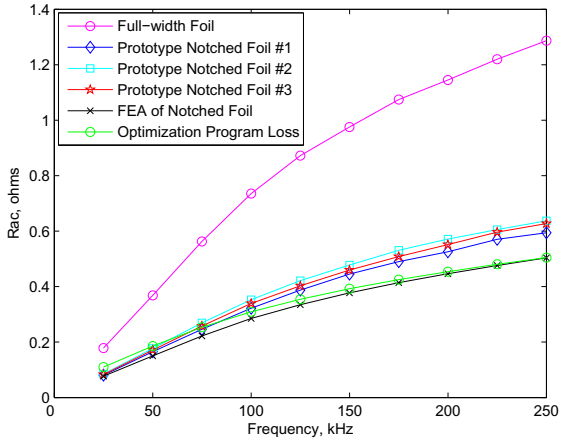

Fig. 5. Experimental results. The resistance of all windings was measured by an impedance analyzer. The full-width foil winding is compared to a notched foil winding optimized for 15% ripple ratio with a notch radius of 6.32 mm. The inductor specifications are given in Table I. The resistance of the notched foil winding was determined by FEA and the optimization method presented here.

gap in the core. As the winding is moved away from the gap, the height of the foil becomes thinner to maintain the same number of layers and insulation thickness. This increases dc resistance, but spreads the current crowding near the gap over a wider area and thus decreases ac resistance [12], [13], [14]. Using FEA, a wide range of spacings were examined. The lowest loss design was determined for each ripple ratio; these designs are included in Fig. 4.

Comparing all the designs in Fig. 4, we see that the foil windings with optimized circular notches are superior to all the alternatives for ripple ratios between 5% and 50%. The range over which circular notches are advantageous is expected to also include ripple ratios above 50%, because even though litz-wire designs with lower loss exist, the designs shown in Fig. 4 are very expensive. For a practical situation, one would want to also compare losses to lower-cost litz-wire designs. The designs with a full-width foil spaced away from the gap perform better than the litz-wire designs for ripple ratios up to 40%. The optimized circular notch designs perform better than the these designs by 4% at a ripple ratio of 10% and by 23% at a ripple ratio of 50%.

For ripple ratios between 5% and 15% the winding loss in the full-width foil is mostly due to the dc resistance with only a small contribution from the ac resistance. For example, at 5% ripple ratio, the loss due to dc resistance is 3.03 W and the loss due to the ac resistance is 0.175 W which accounts for only 5.5% of the total loss. At 15% ripple ratio, the loss due to the ac resistance is 1.7 W which accounts for 36% of total loss. For the notched foil at 5% ripple ratio, the ac loss makes up only 7% of total loss while at 15% ripple ratio ac loss makes up 24% of loss. The higher the ripple ratio, the greater the contribution of ac resistance to total power loss.

E. Verification of Loss Calculation

Several winding designs for the inductor specified in Table I were built to verify the improved performance of the winding configurations proposed here. The model for the winding loss calculations presented here matches the experimental results well. Fig. 5 shows the resistance of a full-width foil and a notched foil optimized for a 15% ripple ratio with a notch radius of 6.32 mm. The ac resistance of the notched winding is between 53% and 56% less for the frequency range under consideration. For the notched foil windings, the measured ac resistance is between 5% and 17% higher than predicted by the model or FEA whereas the measured dc resistance is 2.7% higher than predicted by FEA and 3.6% higher than predicted by the optimization. The total power loss calculated from the measured resistance, for the currents in Table I, is 3.78 W. This is only 1.3% higher than the loss predicted by the loss calculation used by the optimization program.

Several factors were investigated as possible contributors to the small discrepancies observed between the models and the measurements, including the length of the gap in the core, the effects of the winding leads and skewed layers in the notch. Our investigation into the effects of gap length in the core on winding loss showed that it had little effect as expected based on previous work on gap effects [12], [13], [14].

It is important to construct the shape of the notch accurately. Each foil layer must be placed as shown in Fig. 1 to maintain a uniform current distribution on the surface of the notch. When foil layers slip out of alignment, localized current crowding creates areas with high current densities which can increase the winding losses significantly. Using FEA, the effect of the position of the layers closest to the gap on ac resistance was investigated; the results are shown in Fig. 6. At 50 kHz, a 1 mm shift towards the center of the winding by the layer closest to gap (the first layer)

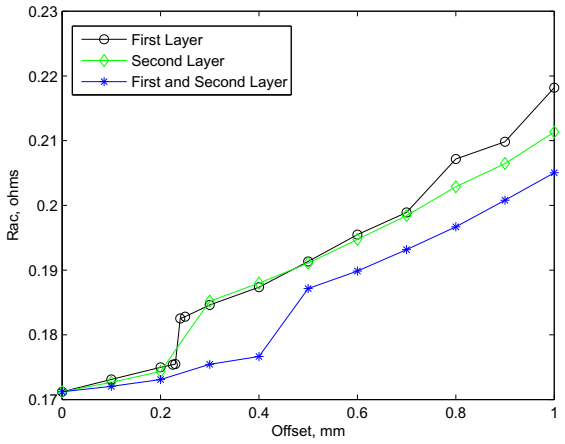

Fig. 6. The ac resistance of foil layers offset from desired position at 50 kHz as determined by FEA. Offset is defined as the distance the layer is shifted away from its ideal position, towards the gap. When the offset is zero, the notch is in the desired position.The first layer is the layer closest the gap in the core. The results of moving both the first and the second layer together are also plotted.

increases the ac resistance of the winding by 22%. As the offset of the first layer increases from zero, the ac resistance increases only slightly until the edge of the first layer lines up or moves beyond the edge of the second layer. Once the first layer moves beyond the edge of the second layer (at 0.3 mm in this case), the ac resistance jumps up by 7.3%. This effect can be seen for both the first and second layers in Fig. 6. The effects of offset of the second layer alone are slightly lower than the first layer, but still have detrimental effects on overall winding resistance when it moves beyond the third layer. We found that once layers move closer to the gap than the layers above them, the ac resistance of the winding can increase by 7% or more.

The placement of the winding leads does have considerable effect on total winding loss but proper placement can avoid problems. The winding leads from the inner end of a notched foil winding should not cut across the notch, but rather should extend out to each side of the winding.

III. Windings for Distributed-Gap Cores

High-frequency currents tend to flow on the surface of a foil winding facing the low-permeability core as shown in Fig. 8. The high-frequency currents are concentrated in the corners of the foil. This phenomenon contributes to the large ac resistance exhibited by full-width foil windings, shown in the top of Fig. 7.

In order to reduce the detrimental current crowding in the corners of a single layer, we propose to cut the foil before winding so as to open space in the corners as shown in Fig. 7. Fig. 7 shows a foil winding with the end of the winding shaped into a semi-circle. Removing copper increases dc resistance somewhat, but by properly selecting the amount of copper removed, we can, as shown below, improve overall performance. Finite element simulations have shown that using an arc or ellipse to define the cut-away area, as shown in the bottom of Fig. 7, results in better performance than do many shapes, but other shapes are still under investigation.

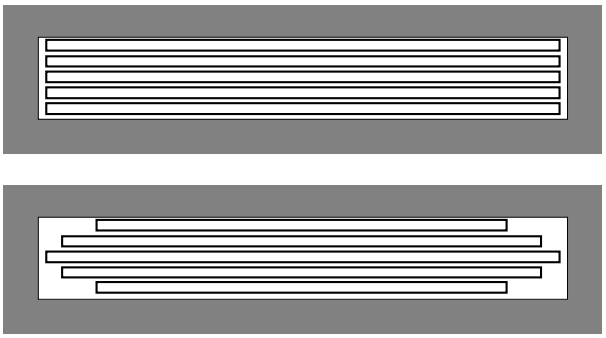

Fig. 7. The common rectangular cross-section of a foil winding in which each layer occupies the entire width of winding window is shown in the top figure. The bottom figure shows a shape optimized foil winding in a distributed-gap core. The core is shown in gray.

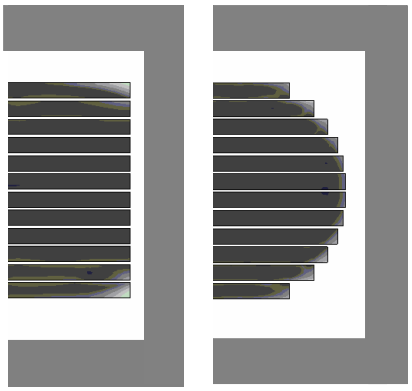

Fig. 8. FEA simulation of current density in full-width foil winding(left figure). FEA simulation of current distribution in a circular shaped foil winding(right figure). The distributed-gap core is shown in gray.

A. Discussion and Verification

The method was tested on an example 38 μH inductor as detailed in Table II. The example inductor used a KoolMu 00K5530E core [15]. Several windings, each with a different cross section, were simulated using FEA and the results are plotted in Fig. 9. The star in Fig. 9 represents the full-width winding. The shape of the winding is varied from the full-width foil to a shape with rounded corners defined either by an ellipse or circle. Fig. 9 shows that as the cut-away area is increased, the ac resistance is reduced while the dc resistance increases only slightly. The distributed gap core creates a nearly one-dimensional field in the winding window. Thus the reduction in ac resistance is small compared to the reductions achieved for high-permeability gapped core windings. However, the shaped foil creates a uniform current distribution as shown in Fig. 8 which reduces the resistance. The shaped foil winding also uses less material.

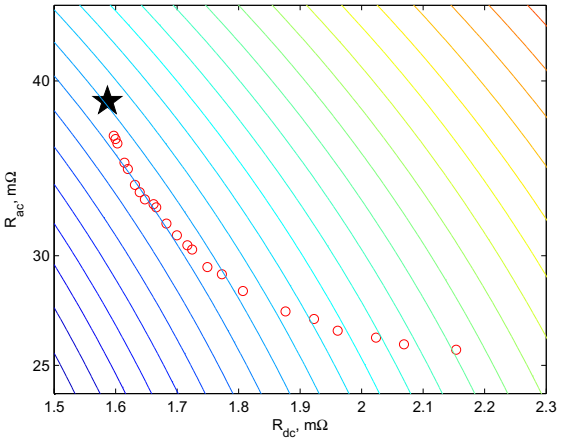

Fig. 9. Ac resistance vs dc resistance for different shaped cross-sections on a distributed-gap core. Each point represents a different shape cross section. The star represents a full-width foil winding. The contour lines are spaced 2% change in total loss apart; the lowest loss is found at the lower-left hand corner and the highest loss is found at the upper-right hand corner of the plot. The lowest loss design has about 3% lower loss than the full cross-section design.

TABLE II

INDUCTOR SPECIFICATIONS

Specification	Value	Units
Inductance	38	uH
Number of Turns, N	12	NA
DC current, I_{dc}	40	A
Peak-to-Peak Ripple Amplitude	20	A
Ripple Frequency	50	kHz

IV. CONCLUSION

Significant reductions in winding losses can be achieved by modifying the shape of the cross section of a foil winding. We have introduced a new loss calculation method that provides improved accuracy for loss calculation in windings with semi-circular cut-outs on gapped cores, as verified by finite-element simulations and experimental results. Optimization using this loss calculation produces designs with up to a factor of two lower losses than either full-width foil windings or litz-wire windings. We have also extended this approach to distributed gap cores. Foil winding shapes for distributed-gap cores were introduced and shown to provide a reduction in power loss.

Foil windings are relatively easy to manufacture compared to solid-wire or litz-wire windings. The new foil winding configurations proposed in this paper do not impose difficult or expensive manufacturing challenges. Since the foil is cut before winding, the only additional step is to cut the edges of the piece of copper to the appropriate dimensions.

V. ACKNOWLEDGEMENTS

Thanks to Weyman Lundquist and Ryan Goldhahn of West Coast Magnetics.

REFERENCES

[1] Jiankun Hu and C. R. Sullivan, "Optimization of shapes for round-wire high-frequency gapped-inductor windings", in *Proceedings of the 1998 IEEE Industry Applications Society Annual Meeting*, 1998, pp. 900–906.

[2] Jiankun Hu and C. R. Sullivan, "Analytical method for generalization of numerically optimized inductor winding shapes", in *30th Annual IEEE Power Electronics Specialists Conference*, 1999, vol. 1, pp. 568–73.

[3] C.R. Sullivan, J.D. McCurdy, and R.A. Jensen, "Analysis of minimum cost in shape-optimized litz-wire inductor windings", in *IEEE 32nd Annual Power Electronics Specialists Conference*, 2001, pp. 1473–8 vol. 3.

[4] A.J. Sinclair and J.A. Ferreira, "Optimal shape for ac foil conductors", in *Prooceedings of PESC 1995 - Power Electronics Specialists Conference*, 1995, vol. 2, pp. 1064 – 1069.

[5] Jennifer D. Pollock and Charles R. Sullivan, "Gapped-inductor foil windings with low ac and dc resistance", in *39th Annual IEEE Industrial Application Society Conference*, 2004.

[6] Charles R. Sullivan and Jennifer D. Pollock, "Low ac resistance foil windings for gapped inductors", March 29, 2004, U.S. Patent Application No. 60/557,268.

[7] The MathWorks, Inc., http://www.mathworks.com, *MATLAB Version 6*, 2000.

[8] Xi Nan and Charles R. Sullivan, "An improved calculation of proximity-effect loss in high-frequency windings of round conductors", in *35th Annual IEEE Power Electronics Specialists Conference*, 2003.

[9] J. H. Spreen, "Electrical terminal representation of conductor loss in transformers", *IEEE Transactions on Power Electronics*, vol. 5, no. 4, pp. 424–9, 1990.

[10] J.C. Lagarias, J.A. Reeds, M.H. Wright, and P.E.Wright, "Convergence properties of the nelder-mead simplex method in low dimensions", in *SIAM Journal on Optimization*, 1998, vol. 9, pp. 112–147.

[11] *Dartmouth Magnetic Component Research Web Site*, http://engineering.dartmouth.edu/inductor.

[12] Jiankun Hu and C. R. Sullivan, "The quasi-distributed gap technique for planar inductors: Design guidelines", in *Proceedings of the 1997 IEEE Industry Applications Society Annual Meeting*, 1997, pp. 1147–1152.

[13] Jiankun Hu and C.R. Sullivan, "Ac resistance of planar power inductors and the quasidistributed gap technique", *IEEE Transactions on Power Electronics*, vol. 16, pp. 558–567, 2001.

[14] Alex Van den Bossche and Vencislav Cekov Valchev, *Inductors and Transformers For Power Electronics*, Dekker/CRC Press, 2005.

[15] *Kool Mu E Cores from Magnetics*, http://www.mag-inc.com/powder/kool_mu_e_cores.asp.